Journal of Marine Science and Technology

Volume 25 | Issue 1 Article 2

BACKGROUND WHITENED TARGET DETECTION ALGORITHM FOR HYPERSPECTRAL IMAGERY

Hsuan Ren
Center for Space and Remote Sensing Research, National Central University, Taoyuan City, Taiwan, R.O.C.

Hsien-Ting Chen
Department of Computer Science and Information Engineering, National Central University, Taoyuan City, Taiwan, R.O.C., slashsabo@gmail.com

Recommended Citation
Ren, Hsuan and Chen, Hsien-Ting (2017) "BACKGROUND WHITENED TARGET DETECTION ALGORITHM FOR HYPERSPECTRAL IMAGERY," *Journal of Marine Science and Technology*: Vol. 25: Iss. 1, Article 2.
DOI: 10.6119/JMST-016-0630-1
Available at: https://jmstt.ntou.edu.tw/journal/vol25/iss1/2

Journal of Marine Science and Technology, Vol. 25, No. 1, pp. 15-22 (2017)
DOI: 10.6119/JMST-016-0630-1

BACKGROUND WHITENED TARGET DETECTION ALGORITHM FOR HYPERSPECTRAL IMAGERY

Hsuan Ren[1] and Hsien-Ting Chen[2]

Key words: Background Whitened Target Detection Algorithm, Anomaly Detection, RX algorithm, synchronization Skewness and Kurtosis method, whitening process.

ABSTRACT

Hyperspectral remotely sensed imagery has undergone rapid advancements recently. Hyperspectral sensors collect surface information with hundreds of channels which results in hundreds of co-registered images. To process this huge amount of data without information of the scene is a great challenge, especially for anomaly detection. Several methods are devoted to this problem, such as the well-known RX algorithm and high-moment statistics approaches. The RX algorithm can detect all anomalies in a single image but it cannot discriminate them. On the other hand, the high-moment statistics approaches use criteria such as Skewness and Kurtosis to find the projection directions recursively, so it is computationally expensive. In this paper, we propose an effective algorithm for anomaly detection and discrimination extended from RX algorithm, called Background Whitened Target Detection Algorithm (BWTDA). It first models the background signature with Gaussian distribution and applies whitening process. After the process, the background will be indepenent-identical-distributed Gaussian in all spectral bands. Then apply Target Detection Process (TDP) to search for potential anomalies automatically and Target Classification Process (TCP) for classifying them individually. The experimental results show that the proposed method can improve the RX algorithm by discriminating the anomalies and outperforming the original high-moment statistics approach in terms of computational time.

I. INTRODUCTION

Hyperspectral imaging spectrometers can collect co-registered image data of the ground in hundreds of spectral bands simultaneously corresponding to different wavelengths. In order to improve the capability of surface materials discrimination and identification, higher spatial resolution and finer spectral resolution spectrometers are generally required. In general each image scene may have several hundred megabytes of digital information. To process such huge data volume without prior information of the background is a very challenging problem.

Anomaly detection has drawn lots of attention lately and is important in surveillance applications. An anomaly usually has small size of a few pixels and has distinct spectral features from its neighborhood with unknown spectral signatures. Therefore, anomaly detection is to find unknown small targets from an unknown background, such as detecting small man-made targets in a large unknown image scene. Several approaches have been proposed for this purpose. For instance, Reed and Yu developed the well-known RX algorithm (Reed and Yu, 1990; Yu et al., 1993) to analyze the image based on the second-order statistics; Ashton used an adaptive Bayesian classifier (Ashton, 1998); Ifarraguerri and Chang's Projection Pursuit (PP) introduced the information divergence to search the best projector for anomaly detection (Ifarraguerri and Chang, 2000); Schweizer and Moura presented a new anomaly detection method based on Gauss-Markov Random Field (GMRF) (Schweizer and Moura, 2001); Chang and Chiang introduced the high-order statistics to hyperspectral image analysis (Chiang et al., 2000; Chiang et al., 2001); Ren presented high-moment statistics approaches based on steepest descent (Ren et al., 2006); Caefer modified the covariance matrix for RX algorithm (Caefer et al., 2008) and Matteoli further improved with the local background covariance matrix (Matteoli et al., 2010); Guo adjusted the weight of the anomalous pixels and the background samples to improve the performance of RX algorithm (Guo et al., 2014). However, these techniques are somewhat time consuming and some of them (such as RX algorithm) can only detect the anomalies without discriminate them. The goal of our research is to develop an efficient algorithm for hyperspectral imagery, which not only detects the anomalies but also can discriminate them.

Since image background is homogeneous, anomalies or small man-made targets can be viewed as outliers in an image scene because their sizes are relatively small and spectral features are very different compared to their surroundings. As a result, anomaly detection in an unknown image scene can be accom-

Paper submitted 12/06/15; revised 06/06/16; accepted 06/30/16. Author for correspondence: Hsien-Ting Chen (e-mail: slashsabo@gmail.com).
[1] Center for Space and Remote Sensing Research, National Central University, Taoyuan City, Taiwan, R.O.C.
[2] Department of Computer Science and Information Engineering, National Central University, Taoyuan City, Taiwan, R.O.C.

plished by searching the deviation from the background distribution. It is known that RX algorithm uses Mahalanobis distance to find anomalies, which is Euclidean distance measure after data whitening process, based on the fact that after the background pixel vectors are whitened, those anomaly pixels become outliers. Since distance measures only record the distances but not the vector directions, they cannot discriminate the outliers from different sources, unlike projection methods. As a result, the RX algorithm detects all the outliers without distinguishing them. In order to separate the anomalies from different sources, we proposed a new method based on subspace projection, called Background Whitened Target Detection Algorithm (BWTDA). It first whitens the background pixel vectors so that the anomalies become outliers. Then Target Detection Process (TDP) of Automatic Target Detection and Classification Algorithm (ATDCA) (Ren and Chang, 2003) is applied to automatically search for potential outliers. It is then followed by Least Squares (LS) method as Target Classification Process (TCP) to classify them based on their spectral information. Since ATDCA is based on subspace projection, it can classify different outliers not only by their distances but also the directions.

The paper is organized as follows. In Section 2, Background Whitened Target Detection Algorithm is introduced to search for anomalies and classify them. The SPECIM V10E data experiments demonstrate the performance of the proposed algorithms based on high-order statistics in Section 3. Finally, conclusions are drawn in Section 4.

II. BACKGROUND WHITENED TARGET DETECTION ALGORITHM

Since in anomaly detection, most pixels are considered as background pixels, the sample covariance matrix of the whole image can be approximately that of background pixels. In this case, if we whitened the image data with the sample covariance matrix, those pixels with large magnitudes, i.e., long distances from origin, are considered as anomalies. Because RX algorithm only records the distance measure, it detects the anomalies without any discrimination. In order to distinguish anomalies made by different materials, an automatic target recognition method called Automatic Target Detection and Classification Algorithm (ATDCA) is adopted. It first searches for potential targets by their spectral information, and then classifies them with least squares approach.

The Background Whitened Target Detection Algorithm (BWTDA) has two stages. The first stage is the data whitening process which centralizes and decorrelates the image data. It is then followed by ATDCA to search and classify anomalies by their spectrum into different images. The detail method is described as following:

1. Data Whitening Process

Assume that there are N data points $\{\mathbf{x}_n\}_{n=1}^{N}$ each with dimensionality L and $\mathbf{X} = [\mathbf{x}_1\ \mathbf{x}_2\ \ldots\ \mathbf{x}_N]$ is an $L \times N$ data matrix. In order to make the variance unity, centering the original data matrix is required. The data is centralized by removing the mean vector from the data set with $\hat{\mathbf{X}} = \mathbf{X} - \boldsymbol{\mu} \cdot \mathbf{1}^T = [\mathbf{x}_1 - \boldsymbol{\mu}, \mathbf{x}_2 - \boldsymbol{\mu}, \ldots, \mathbf{x}_N - \boldsymbol{\mu}]$, where $\boldsymbol{\mu} = \frac{1}{N}\sum_{n=1}^{N}\mathbf{x}_n$ is the sample mean vector and $\mathbf{1} = [\underbrace{1 1 \cdots 1}_{N}]^T$ is column vector with all elements equal to 1. Then the data is decorrelated by applying the decorrelation transformation described as follows.

Assume that $\{\lambda_i\}_{i=1}^{L}$ are the eigenvalues of the sample covariance matrix $\boldsymbol{\Sigma} = \hat{\mathbf{X}}\hat{\mathbf{X}}^T$ and $\{\mathbf{v}_i\}_{i=1}^{L}$ are their corresponding eigenvectors. The covariance matrix can be decomposed into Eq. (1):

$$\mathbf{V}^T\boldsymbol{\Sigma}\mathbf{V} = \boldsymbol{\Lambda} \tag{1}$$

where $\mathbf{V} = [\mathbf{v}_1\mathbf{v}_2 \ldots \mathbf{v}_L]$ is a matrix made up of the eigenvectors with the property $\mathbf{V}^T = \mathbf{V}^{-1}$ and $\boldsymbol{\Lambda} = diag\{\lambda_i\}_{i=1}^{L}$ is a diagonal matrix with eigenvalues in the diagonal. Let $\boldsymbol{\Lambda}^{-1/2} = diag\{1/\sqrt{\lambda_i}\}_{i=1}^{L}$ and apply it to both sides of Eq. (1) results in

$$\mathbf{V}\boldsymbol{\Lambda}^{-1/2}\mathbf{V}^T\boldsymbol{\Sigma}\mathbf{V}\boldsymbol{\Lambda}^{-1/2}\mathbf{V}^T = \mathbf{I} \tag{2}$$

From Eq. (2), we obtain the desired sphering matrix A, given by

$$\mathbf{A} = \mathbf{V}\boldsymbol{\Lambda}^{-1/2}\mathbf{V}^T \tag{3}$$

so that $\mathbf{A}^T\boldsymbol{\Sigma}\mathbf{A} = \mathbf{I}$. The new data set becomes $\mathbf{Y} = [\mathbf{y}_1\mathbf{y}_2 \ldots \mathbf{y}_N] = \mathbf{A}^T(\mathbf{X} - \boldsymbol{\mu} \cdot \mathbf{1}^T)$, which has zero mean and independent-identical-distributed (iid) with unity variance. The process with Eqs. (1)-(3) is called sphering, also known as data whitening process.

It is worth noting that the famous RX algorithm uses the pixel currently being processed as the matched signal, therefore the matched signal used in the RX varies pixel by pixel. Since the RX uses the sample covariance matrix to take into account the sample spectral correlation, it performs the same task as does the Mahalanobis distance:

$$RX(\mathbf{r}) = (\mathbf{r} - \boldsymbol{\mu})^T\boldsymbol{\Sigma}^{-1}(\mathbf{r} - \boldsymbol{\mu}) \tag{4}$$

If the covariance matrix is substituted by whitening matrix A, then Eq. (4) can be rewritten as Euclidean distance to origin after data whitening process:

$$RX(\mathbf{r}) = [\mathbf{A}(\mathbf{r} - \boldsymbol{\mu})]^T[\mathbf{A}(\mathbf{r} - \boldsymbol{\mu})] \tag{5}$$

2. Automatic Target Detection and Classification Algorithm

After the data whitening process, the next task is to search

and classify potential anomalies. The ATDCA is developed for the purpose where we assume no a *priori* knowledge is available. Since there is no information about the initial target, in order for the Target Detection Process (TDP) to be fully automated, the initial target must be generated in such a fashion that no prior knowledge is used. One way is to select a target pixel vector with the maximum length, namely, $\mathbf{T_0} = \arg\left\{\max_{\mathbf{r}}[\mathbf{r}^T\mathbf{r}]\right\}$. By doing so, $\mathbf{T_0}$ may not necessarily be a target. It may be a strong interferer. Then ATDCA employs an orthogonal subspace projector $P^{\perp}_{\mathbf{T}_0} = \mathbf{I} - \mathbf{T}_0\left(\mathbf{T}_0^T\mathbf{T}_0\right)^{-1}\mathbf{T}_0^T$ to project all image pixel vectors into the orthogonal complement space, denoted by $\langle\mathbf{T_0}\rangle^{\perp}$ that is orthogonal to the space. The maximum length of a pixel vector in $\langle\mathbf{T_0}\rangle^{\perp}$ corresponds to the most distinct features from $\mathbf{T_0}$ in the sense of orthogonal projection. This pixel vector will be selected as a first potential target denoted by $\mathbf{T_1} = \arg\left\{\max_{\mathbf{r}}[\mathbf{r}^T P^{\perp}_{\mathbf{T}_0}\mathbf{r}]\right\}$. Then another orthogonal subspace projector $P^{\perp}_{(\mathbf{T_0}\mathbf{T_1})}$ is applied again to the original image by projecting all image pixel vectors to the space, $\langle\mathbf{T_0}, \mathbf{T_1}\rangle^{\perp}$ that is orthogonal to both $\mathbf{T_0}$ and $\mathbf{T_1}$. Once again, the pixel vector with maximum length in $\langle\mathbf{T_0}, \mathbf{T_1}\rangle^{\perp}$ will be selected as a second target denoted by $\mathbf{T}_2$. The above procedure will be repeated again to find the third target $\mathbf{T}_2$, the fourth target $\mathbf{T}_4$, etc. until the terminating criterion is satisfied. The stopping rule is based on the orthogonal correlation between the data set and the projection operator $P^{\perp}_{(\mathbf{T}_0 \ldots \mathbf{T}_i)}$. Based on orthogonal subspace projection, the value $\max[\mathbf{r}^T P^{\perp}_{(\mathbf{T}_0 \ldots \mathbf{T}_i)}\mathbf{r}]$ is monotonically decreasing at i. When it is lower than a preset threshold, the TDP is terminated. Finally, combining the TDP with the LS classifier, ATDCA can be implemented as follows:

(1) Select $\mathbf{T_0} = \arg\left\{\max_{\mathbf{r}}[\mathbf{r}^T\mathbf{r}]\right\}$. Let $i = 0$.

(2) Find orthogonal projections of all image pixels with respect to $\mathbf{T_0}$ by applying $P^{\perp}_{\mathbf{T}_0}$ to all image pixel vectors $\mathbf{r}$ in the image. If $\max[\mathbf{r}^T P^{\perp}_{(\mathbf{T}_0 \ldots \mathbf{T}_i)}\mathbf{r}] < \varepsilon$, go to step 6.

(3) Let the first potential target denoted by

$$\mathbf{T_1} = \arg\left\{\max_{\mathbf{r}}[\mathbf{r}^T P^{\perp}_{\mathbf{T}_0}\mathbf{r}]\right\}, i = i + 1 \text{ and continue.}$$

(4) If $\max[\mathbf{r}^T P^{\perp}_{(\mathbf{T}_0 \ldots \mathbf{T}_i)}\mathbf{r}] > \varepsilon$, let the i-th potential target $\mathbf{T_1} = \arg\left\{\max_{\mathbf{r}}[\mathbf{r}^T P^{\perp}_{(\mathbf{T}_0 \ldots \mathbf{T}_{i-1})}\mathbf{r}]\right\}$.

(5) Repeat (4) until $\max[\mathbf{r}^T P^{\perp}_{(\mathbf{T}_0 \ldots \mathbf{T}_i)}\mathbf{r}] < \varepsilon$.

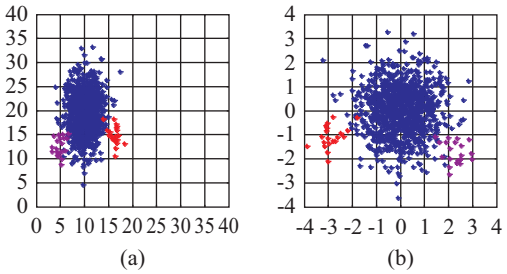

Fig. 1. (a) Original data distribution. (b) Whitening result.

(6) Use LS to classify all potential anomalies individually.

III. EXPERIMENTAL RESULS

In this section, we first present a computer simulation to illustrate the data whitening and compare the mechanism of the RX and BWTDA, followed by real data experiment from SPECIM V10E data to evaluate the effectiveness of the BWTDA algorithm.

1. Computer Simulation (Two-Dimensional Data)

A two-dimension data set is simulated with 1000 blue background pixels with mean $\mu_B = [10, 20]^T$ 4 and covariance matrix $\Sigma_B = \begin{bmatrix} 4 & 0 \\ 0 & 16 \end{bmatrix}$ and 20 pixels for each of two types of anomalies with same covariance matrix $\Sigma = \begin{bmatrix} 1 & 0 \\ 0 & 4 \end{bmatrix}$ and mean $\mu_1 = [16, 15]^T$ in red, $\mu_2 = [5, 12]^T$ in magenta respectively, shown in Fig. 1(a). Since the data has very few anomaly pixels, the mean and covariance matrix of the data set should be close to those of the background. After applying the whitening process by removing the mean and de-correlating the data as Eq. (3), the background pixels will distribute as a sphere, and the anomalies will be far from the origin.

When RX algorithm is applied to detect anomaly, as shown in Eq. (5), it actually calculates the square of Euclidean distance from the origin after the whitening process. If the distance is beyond a preset threshold, it will be considered as anomaly pixel. As shown in Fig. 2(a), RX can detect those red and magenta pixels, but it cannot distinguish them as two different types of anomalies.

The original ATDCA can also search for potential targets in the unknown background by Target Detection Process (TDP). But it will select background pixels first as potential targets since their signals are stronger than that of anomaly pixels in this simulation in Fig. 2(b). On the other hand, if the ATDCA is applied to the whitened data, after the background pixels have been centered to the origin and decorrelated, the TDP can easily find these two types of anomalies as two different potential targets in Fig. 2(c).

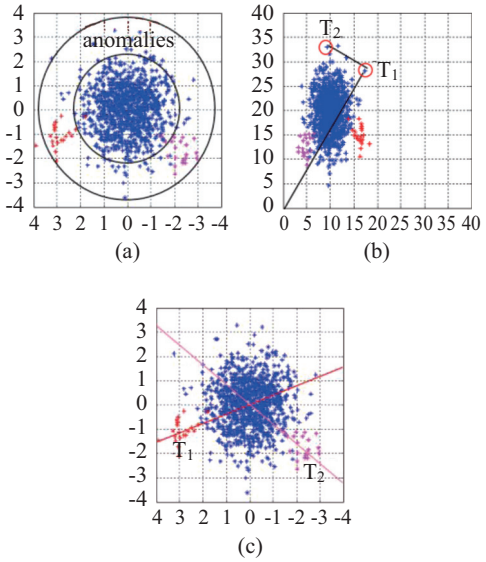

Fig. 2. Data distribution from using (a) RX algorithm, (b) original ATDCA and (c) BWTDA.

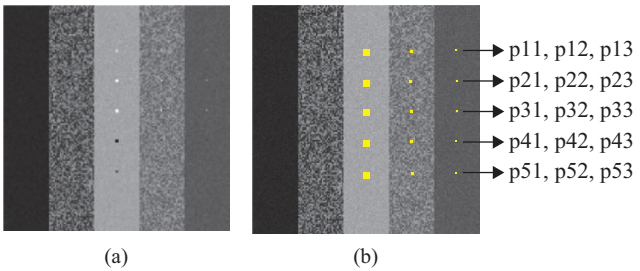

Fig. 3. (a) Simulation image scene (band 107). (b) Five types of panels with three sizes in the image.

2. Computer Simulation (Multi-Dimensional Data)

In this section, we demonstrate the performance of our method with simulated multi-dimensional data. The spectra for this experiment were chosen from the United States Geologic Survey (USGS) digital spectral library (Clark et al., 1993). They were measured by Airborne Visible InfraRed Imaging Spectrometer (AVIRIS) with 224 bands in the range of 0.4-2.5 μm, which resulting 10 nm spectral resolution.

The size of simulated image is 150 × 150. Three materials are selected as background signatures, which are desert varnish, dry grass, and maple leaves. The image scene of the 107th band is shown in Fig. 3(a). The pixels in columns 1-30, 61-90, 121-150 are pure pixels of desert varnish, dry grass and maple leaves respectively, each having 150 × 30 pixels. The pixels 31-60 are linearly mixed by desert varnish and dry grass and in column 91-120 are desert varnish and maple leaves. The percentages of each signature are randomly select from uniform distribution and the sum of two mixed percentages equals to one. Five signatures are chosen as 15 anomaly targets and arranged in 5 rows and 3 columns, indicates as p_{ij} with row indexed by i = 1, …, 5 and column indexed by j = 1, …, 3. From rows 1 to 5 are hydrogrossular, muscovite, sodium bicarbonate, black brush, Russian olive. From columns 1 to 3 are targets with 2 × 2 pure pixels, one pure pixel, and one sub-pixel which is linearly mixed with 50% of targets and 50% of backgrounds. Correlated Gaussian noises with SNR = 6 and correlation coefficient as 0.7 are added to the data. The definition of signal-to-noise ratio (Chang, 2003) is

$$\mathrm{SNR} = \frac{\frac{1}{2} \times \frac{1}{N \times \sum_{i=1}^{N} S_i}}{\delta}$$

S_i: the value of the pixel, δ: the variance of the noise

Table 1. Performance of ATDCA, BWTDA, and SK method.

target \ algorithm	ATDCA	BWTDA	SK method
hydrogrossular	4	2	2
muscovite	7	3	3
sodium bicarbonate	2	1	1
black brush	5	4	4
Russian Olive	10	6	5
Computing time	**2.5** sec.	**1.8** sec.	**7** sec.

Fig. 3(b) shows the exact locations of those 15 targets. The experiment is programmed in MATLAB on the computer with Intel i-3 CPU and 8G RAM.

Table 1 shows the computational time of three methods: ATDCA, BWTDA, and SK method (Ren et al., 2006). SK method bases on the concept that if background cannot be modeled as Gaussian, then irregular objects in background can be detected by applying the high-order statistics with skewness or kurtosis as a criterion to find the optimal projection direction such that the projected data has the maximal normalized central moments. By projecting the original data onto a certain direction, anomalies can be detected.

Table 1 shows that for the high-dimensional data, ATDCA still selects background pixels as the first potential target. This situation is similar to the result using 2D data in section 3.1. Five anomalies, hydrogrossular, muscovite, sodium bicarbonate, black brush and Russian olive, are detected in the 4th, 7th, 2nd, 5th, 10th potential targets by ATDCA. Because BWTDA whitened the data first, the anomalies were found in the first projection. Five anomalies are detected in the 2nd, 3rd, 1st, 4th, 6th potential targets respectively. SK method also shows the good result, and five anomalies are detected in the 2nd, 3rd, 1st, 4th, 5th potential targets. But SK method takes more time to find the projection direction iteratively. The LS results of ATDCA, BWTDA, and SK method are shown in Figs. 4(b), 5(b), and 6(b).

3. Real Data Analysis

The scene used in the experiments was taken in National

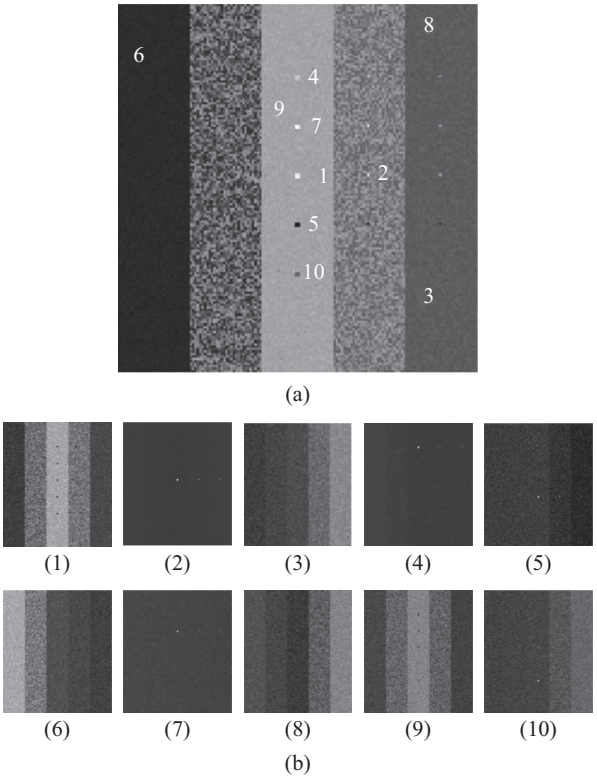

Fig. 4. (a) The ATDCA result of simulation image. (b) LS result.

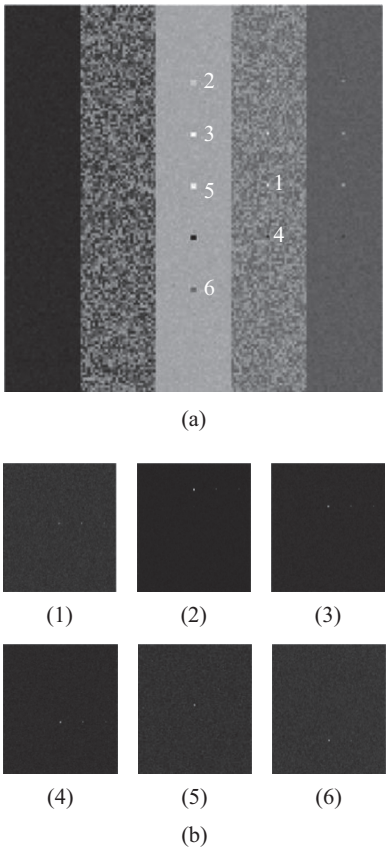

Fig. 5. (a) The BWTDA result of simulation image. (b) LS result.

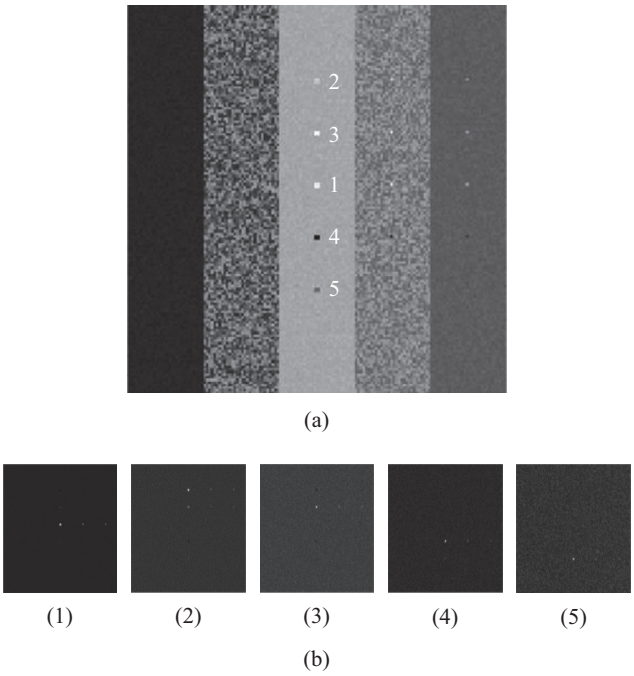

Fig. 6. (a) The potential target anomalies detected by SK method in the order as numbered. (b) Classification results.

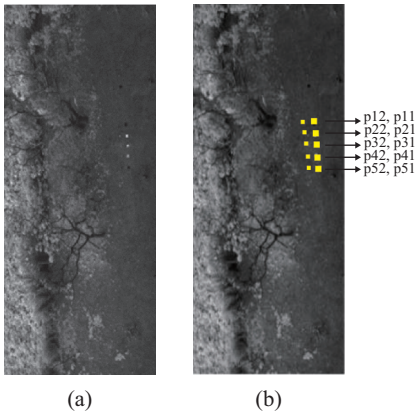

Fig. 7. (a) SPECIM V10E image scene. (b) Five types of panels with two sizes in the image.

Central University using SPECIM V10E sensor. It is a hyperspectral sensor of spectral coverage 0.4-1.0 μm at resolution 3 nm with total 204 bands. The sensor is mounted on a building at 25 meters above ground and the average ground sampling distance (GSD) is 10 cm. The low signal-to-noise-ratio (SNR) bands: 60, 129, 130 and 188 have been removed. Fig. 7(a) shows the image scene of size 325 × 165 in band 117 and Fig. 7(b) provides the exact locations of 10 targets of interest in the scene. These target panels are located on the right field and arranged in a 5 × 2 matrix. Each element in this matrix is a square panel and denoted by p_{ij} with row indexed by $i = 1, \ldots, 5$ and column indexed by $j = 1, 2$. For each row $i = 1, \ldots, 5$, the two panels p_{i1}, p_{i2} were made by the same material, and they are paper,

Fig. 8. RX results show the anomalies including all five rows of panels.

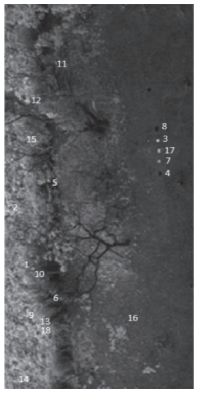

(a)

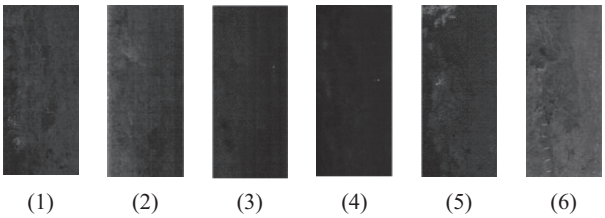

(1) (2) (3) (4) (5) (6)

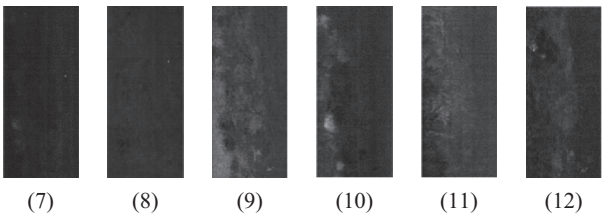

(7) (8) (9) (10) (11) (12)

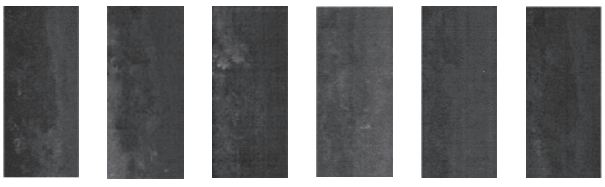

(13) (14) (15) (16) (17) (18)

(b)

Fig. 9. (a) The original ATDCA result. (b) LS result.

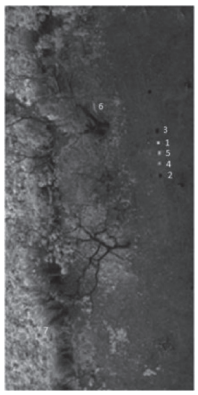

(a)

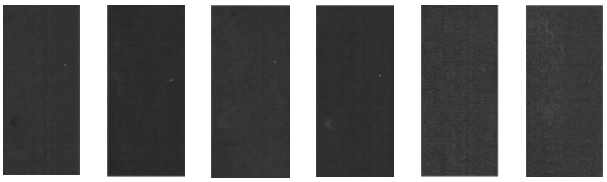

(1) (2) (3) (4) (5) (6)

(b)

Fig. 10. (a) BWTDA result. (b) LS result.

polyester, nylon polyvinylchloride, and cotton. For each column $j = 1, 2$, the five panels p_{1j}, p_{2j}, p_{3j}, p_{4j}, p_{5j} have the same size but were made by five different materials. The sizes of the panels in the first and second columns are 21×21 and 7×7 cm respectively. In summary, the 10 panels comprise five different materials and two different sizes. The ground truth of the image scene provides the precise spatial coordinates of these 10 panels. The 10 cm-spatial resolution indicates that the panels in the first column have pure pixels, while panels in the second column are only in subpixel level.

When RX algorithm is applied to this image scene, in Fig. 8, all five rows of panels are detected in one single image. But those anomalies of different materials cannot be distinguished by RX algorithm.

The original ATDCA uses TDP to search for potential targets. When the stopping criterion is met, 18 potential targets are found as shown in Fig. 9(a). Among these potential targets, the panels in row 1 to 5 are found in the 8^{th}, 3^{rd}, 17^{th}, 7^{th} and 4^{th} targets respectively. Although all those anomalies can also be successfully classified in the corresponding images in Fig. 9(b), the other 13 potential ones are from the background pixels. The anomalies classification results in (3), (4), (7), (8), (17) in Fig. 9(b) still contains some information in the background. We need search for at least 17 potential targets to find all the anomalies.

The BWTDA adopt whitening process before apply ATDCA. In Fig. 10(a), all five rows of panels are detected in 3^{rd}, 1^{st}, 5^{th}, 4^{th} and 2^{nd} potential targets respectively and all can be clearly classified in the corresponding images in Fig. 10(b). Although

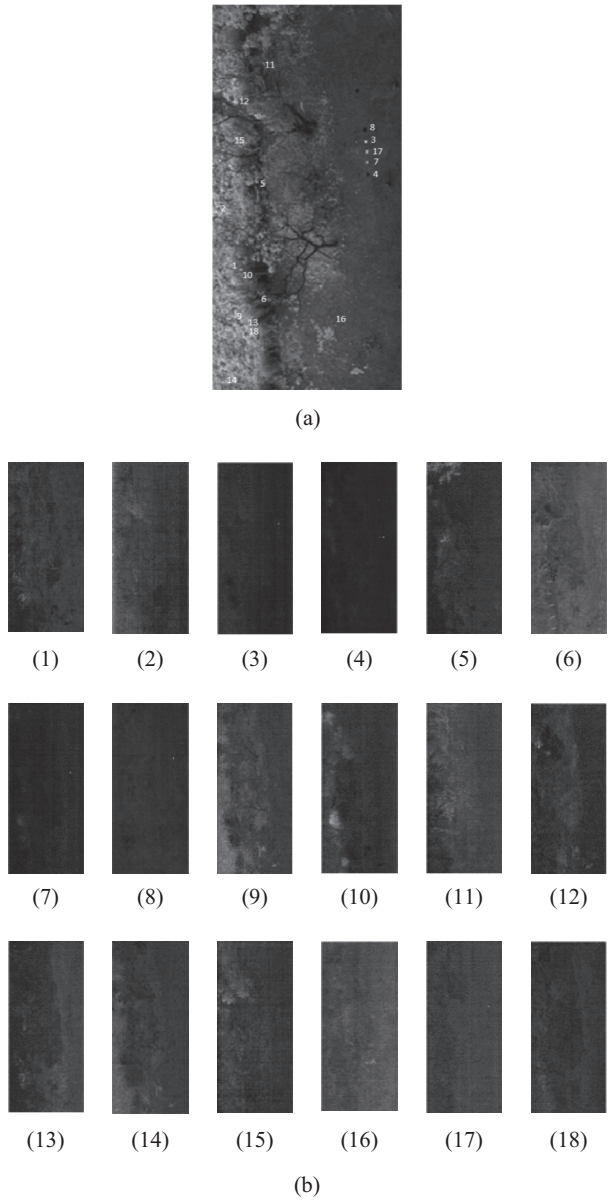

Fig. 11. (a) The potential target anomalies detected by SK method in the order as numbered. (b) Classification results.

the TDP stops with 6 potential targets found, all the different types of anomalies can be individually identified in the first 5 potential ones. It is worth noting that since the background signature have been whitened, i.e., mean-removed and uncorrelated, those background pixels after projection are very close to zero, so only the anomalies are detected.

Like the simulation in 3.2, BWTDA finds the anomalies on the first few searches and shows better results than ATDCA. It is worth noting that the SK method detects panel 2, 3, 4 in the first projection because polyester, nylon, polyvinylchloride are all considered as artificial fiber. The signature paper was found on the 11th projection and took 46 seconds to detect all five signatures as shown in Table 2. Fig. 11 shows the results of SK method.

Table 2. Performance of ATDCA, BWTDA, SK method on the real image.

algorithm / target	ATDCA	BWTDA	SK method
paper	8	3	11
polyester	3	1	1
nylon	17	5	1
polyvinylchloride	7	4	1
cotton	4	2	2
Computing time	**5** sec.	**3** sec.	**46** sec.

IV. CONCLUSIONS

In this paper, a new anomaly detection and discrimination method based on second-order statistics in conjunction with orthogonal subspace projection is introduced. Since image background is homogeneous, anomalies or small man-made targets can be viewed as outliers in an image scene because their sizes are relatively small and spectral features are very different compared to their surroundings. The Background Whitened Target Detection Algorithm (BWTDA) combined two processes to detect and discriminate the anomalies. It first whitened the background pixel vectors so that the anomalies become outliers. Then we use Automatic Target Detection and Classification Algorithm (ATDCA) to automatically search for potential outliers and then classify them based on their spectral information. As a result, BWTDA can effectively detect and discriminate different types of anomalies by their spectral information while the RX algorithm can only detect all anomalies in one image without distinguish them. Since RX algorithm can be considered as Euclidean distance measure after data whitening, BWTDA can be viewed as an expansion of RX by including the orthogonal subspace projection. Therefore, BWTDA is an effective and efficient anomaly detection method based on second-order statistics.

REFERENCES

Ashton, E. A. (1998). Detection of subpixel anomalies in multispectral infrared imagery using an adaptive Bayesian classifier. IEEE Trans. on Geoscience and Remote Sensing 36, 506-517.

Caefer, C. E., J. Silverman, O. Orthal, D. Antonelli, Y. Sharoni and S. R. Rotman (2008). Improved covariance matrix for point target detection in hyperspectral images. Opt. Eng. 47(7), 076402.

Chang, C.-I. (2003). Hyperspectral Imaging: Techniques for Spectral Detection and Classification. Springer, USA.

Chiang, S. S., C.-I. Chang and I. W. Ginsberg (2000). Unsupervised hyperspectral image analysis using independent components analysis. IEEE 2000 International Geoscience and Remote Sensing Symposium, Hawaii, USA, 4-27.

Chiang, S. S., C.-I. Chang and I. W. Ginsberg (2001). Unsupervised target detection in hyperspectral images using projection pursuit. IEEE Trans. on Geoscience and Remote Sensing 39, 1380-1391.

Clark, R. N., G. A. Swayze, A. J. Gallagher, T. V. V. King and W. M. Calvin (1993). The U. S. Geological Survey, Digital Spectral Library: Version 1 (0.2 to 3.0 um). Geological Survey (U.S.) Open-File Report, 93-592.

Guo, Q., B. Zhang, Q. Ran, L. Gao, J. Li and A. Plaza (2014). Weighted-RXD and Linear Filter-Based RXD: Improving Background Statistics Estimation for Anomaly Detection in Hyperspectral Imagery. IEEE Journal of Selected Topics in Applied Earth Observations and Remote Sensing 7, 2351-2366.

Ifarraguerri, A. and C.-I. Chang (2000). Unsupervised hyperspectral image analysis with projection pursuit. IEEE Trans. on Geoscience and Remote Sensing 38, 2529-2538.

Matteoli, S., M. Diani and G. Corsini (2010). Improved estimation of local background covariance matrix for anomaly detection in hyperspectral images. Opt. Eng. 49(4), 046201.

Reed, I. S. and Y. Xiaoli (1990). Adaptive multiple-band CFAR detection of an optical pattern with unknown spectral distribution. IEEE Trans. on Acoustic, Speech and Signal Processing 38, 1760-1770.

Ren, H. and C.-I. Chang (2003). Automatic Target Recognition in Hyperspectral Imagery. IEEE Trans. Aerospace and Electronic Systems 39, 1232-1249.

Ren, H., Q. Du, J. Wang, C.-I. Chang, J. O. Jensen and J. L. Jensen (2006). Automatic Target Recognition for Hyperspectral Imagery Using High Order Statistics. IEEE Trans. Aerospace and Electronic Systems 42, 1372-1385.

Schweizer, M. and J. M. F. Moura (2001). Efficient detection in hyperspectral imagery. IEEE Trans. on Image Processing 10, 584-597.

Yu, X., I. S. Reed and A. D. Stocker (1993). Comparative performance analysis of adaptive multispectral detectors. IEEE Trans. On Signal Processing 41, 2639-2656.